Published in final edited form as:

IEEE Trans Netw Sci Eng. 2018 ; 5(1): 55–64. doi:10.1109/TNSE.2017.2730261.

Pattern Formation over Multigraphs

Andras Gyorgy [Member IEEE] and **Murat Arcak [Fellow IEEE]**

Department of Electrical Engineering and Computer Sciences, University of California, Berkeley, CA, 94720 USA

Abstract

Two of the most common pattern formation mechanisms are Turing-patterning in reaction-diffusion systems and lateral inhibition of neighboring cells. In this paper, we introduce a broad dynamical model of interconnected modules to study the emergence of patterns, with the above mentioned two mechanisms as special cases. Our results do not restrict the number of modules or their complexity, allow multiple layers of communication channels with possibly different interconnection structure, and do not assume symmetric connections between two connected modules. Leveraging only the static input/output properties of the subsystems and the spectral properties of the interconnection matrices, we characterize the stability of the homogeneous fixed points as well as sufficient conditions for the emergence of spatially non-homogeneous patterns. To obtain these results, we rely on properties of the graphs together with tools from monotone systems theory. As application examples, we consider patterning in neural networks, in reaction-diffusion systems, and contagion processes over random graphs.

Index Terms

Nonlinear dynamics; pattern formation; large-scale systems; networks; multigraphs

1 Introduction

Spatial pattern formation plays a fundamental role in the development of complex self-organized systems, such as multi-cellular organisms [1], [2]. The vast majority of theoretical results about the emergence of patterns focus on diffusion-driven instabilities, the so-called Turing-patterning in both biological [3], [4], [5], [6], [7] and abiological systems [8], [9]. However, patterning is also faciliated by mechanisms without any diffusible molecules. For instance, Turing patterns can appear in systems made of immobile agents as a result of differential growth [10], or alternatively, in the case of lateral inhibition in the Notch pathway where neighboring cells inhibit each other from converging on the same fate [1], [11], [12], [13], [14]. Thus, there is growing attention targeted at understanding pattern formation mechanisms other than Turing-patterning.

Studies of patterning either focus on the continuous case with partial differential equations, or consider network analogues: interconnected dynamical systems where nodes represent systems and edges stand for interconnections (e.g., ecological metapopulations [15], [16], spreading of infections over transportation networks [17], [18], [19], diffusively coupled chemical reactors or cells [11], [20], [21], [22], [23]). Since the high-dimension of the

resulting problem renders the analysis difficult, studies so far mainly considered small networks comprising only a few nodes, and resorted to numerical simulations in the case of large-scale networks [11], [13], [22], [23], [24].

To characterize pattern formation in large-scale networks, we view the network as the interconnection of input/output models [25], [26]. Inputs and outputs correspond to, for instance, the concentration of species used for communication among cells, and the interconnection structure is encoded with directed and weighted graphs $P^{(1)}, \ldots, P^{(m)}$, one for each layer of communication channels. Nodes represent modules (e.g., cells in reaction-diffusion systems), edges stand for connection between two nodes, and weights represent the strength of this connection. In addition to studying the stability of the homogeneous fixed points, this formulation allows us to characterize sufficient conditions for the emergence of spatially non-homogeneous patterns irrespective of network complexity.

Recent efforts focusing on pattern formation over directed graphs [27], [28] and multigraphs [28], [29], [30], [31] share a common characteristic: the matrices describing coupling among nodes are the Laplacian operators associated with the network structures, yielding $P^{(k)}$ with zero row-sum. While this assumption is appropriate in the context of diffusion-driven instabilities, it does not permit the study of pattern formation propelled by mechanisms without diffusible molecules, e.g., in the case of lateral inhibition $P^{(k)}$ is row-stochastic (studied in [25], [26] when $P^{(k)}$ are identical and symmetric).

Considering the above, the novelty of this paper is that it focuses on pattern formation over large-scale multigraphs, with directed edges, and without restriction on the row-sum of $P^{(k)}$. Therefore, our results (1) apply to networks where communication among nodes occurs over multiple layers of channels, with possibly different interconnection structures (e.g., two nodes can be connected in one layer and disconnected in another); (2) allow for asymmetric communication among nodes (e.g., one node can have an effect on another without any effect from the other); and (3) capture a wide array of mechanisms leading to patterning (diffusion-driven instability and lateral inhibition both emerge as special cases). Additionally, while the above studies (except for [26]) only focus on the instability of the homogeneous fixed points, we also reveal sufficient conditions for the emergence of non-homogeneous patterns and characterize their location relative to the homogeneous fixed points. Although our main motivation is understanding pattern formation in cellular systems, our results characterize the emergence of patterns in networked systems over directed multigraphs without restrictions to biological systems.

This paper is organized as follows. We first present the mathematical model considered for studying the emergence of patterns over directed multigraphs, together with the main questions of the paper and with the notation and technical assumptions. After focusing on the existence of the homogeneous fixed points, we consider pattern formation over networks with a single layer of communication channels, then generalize the results to the case of multigraphs with multiple layers of communication channels. Finally, we illustrate the implications of the results through application examples considering neural networks, reaction-diffusion systems, and contagion processes over random graphs.

2 Mathematical Model and Notation

Consider a network of identical dynamical systems $i = 1, 2, \ldots, N$, each described by the model

$$\begin{aligned} \dot{x}_i &= f(x_i, u_i), \\ y_i &= h(x_i), \end{aligned} \qquad (1)$$

where $x_i \in \mathbb{R}^n$ denotes the state of system i, and $u_i \in \mathbb{R}^m$ and $y_i \in \mathbb{R}^m$ represent the input and output of this system, respectively, where $u_i = \begin{pmatrix} u_i^{(1)} & \ldots & u_i^{(m)} \end{pmatrix}^T$ and $y_i = \begin{pmatrix} y_i^{(1)} & \ldots & y_i^{(m)} \end{pmatrix}^T$. Introduce x, u and y as the concatenations of x_i, u_i and y_i for $i = 1, 2, \ldots, N$, respectively, and define $u^{(k)} := \begin{pmatrix} u_1^{(k)} & \ldots & u_N^{(k)} \end{pmatrix}^T$ and $y^{(k)} := \begin{pmatrix} y_1^{(k)} & \ldots & y_N^{(k)} \end{pmatrix}^T$.

We consider interactions among subsystems of the form

$$u^{(k)} = P^{(k)} y^{(k)} \quad k = 1, \ldots, m, \qquad (2)$$

where the entry $p_{i,j}^{(k)}$ of the matrix $P^{(k)} \in \mathbb{R}^{N \times N}$ represents the strength of the effect of subsystem j on subsystem i through the k^{th} channel. Therefore, we represent the network by a set of m directed and connected graphs $(V, P^{(k)})$, where V and $P^{(k)}$ denote the set of vertices and the weighted adjacency matrix (assumed to be irreducible), respectively.

In this paper, we study the fixed points of (1)–(2). When does the homogenous fixed points become unstable, setting the stage for patterning? When do spatially non-homogenous patterns emerge? By grouping modules that share the same fate, is it possible to reduce the complexity of the analysis?

While addressing these questions, we consider various subsets of the following main assumptions:

- **(A1)** both $f(\cdot, \cdot)$ and $h(\cdot)$ are continuously differentiable;
- **(A2)** for all $u \in \mathbb{R}^m$ the set of equations $0 = f(x, u)$ has a solution denoted by $x =: S(u)$, in which case we define $T(u) := h(S(u))$;
- **(A3)** $\left.\frac{\partial f(x,u)}{\partial x}\right|_{(S(u),u)}$ is Hurwitz for all $u \in \mathbb{R}^m$;
- **(A4)** the maps $S : \mathbb{R}^m \to \mathbb{R}^n$ and $T : \mathbb{R}^m \to \mathbb{R}^m$ are continuously differentiable;
- **(A5)** $T(\cdot)$ is bounded and $\frac{\partial T(u)}{\partial u}$ is sign-stable (i.e., with $T^{(i)}(\cdot)$ denoting the i^{th} entry of $T(\cdot)$ we have that $\frac{\partial T^{(i)}(u)}{\partial u^{(j)}} \leq 0$ or $\frac{\partial T^{(i)}(u)}{\partial u^{(j)}} \geq 0$ for all u and $i, j = 1, \ldots, m$);

(A6) $P^{(k)}\mathbf{1}_N = p^{(k)}\mathbf{1}_N$ for some $p^{(k)} \in \mathbb{R}$ for $k = 1, \ldots, m$ (constant row-sum);

(A7) $P^{(1)}, \ldots, P^{(m)}$ commute and are diagonalizable (when $m > 1$).

Throughout the paper, we drop the superscript when $m = 1$. Furthermore, let e_i denote the i^{th} unit vector and write $M \leq 0$ and $M \geq 0$ to denote that all entries of M are non-positive and non-negative, respectively. Finally, $\rho(M)$ and $s(M)$ denote the spectral radius and the largest real part of the eigenvalues of M, respectively, whereas diag(v) defines the diagonal matrix composed of the elements of the vector v.

3 Results

Before studying the emergence of patterns, we focus on the existence of homogeneous fixed points. To this end, we first present an input/output formulation for studying the fixed points of (1)–(2), which will be used throughout the paper.

Lemma 1: *Assume that (A2) holds. If* $u_i^{(k)}$ *for* $i = 1, \ldots, N$ *and* $k = 1, \ldots, m$ *satisfy*

$$\begin{pmatrix} u_1^{(k)} \\ \vdots \\ u_N^{(k)} \end{pmatrix} = P^{(k)} \begin{pmatrix} T^{(k)}(u_1) \\ \vdots \\ T^{(k)}(u_N) \end{pmatrix}, \quad (3)$$

then $x_i = S(u_i)$ *is a fixed point of* (1)–(2). *Conversely, if* $S(\cdot)$ *in (A2) is unique and* x *is a fixed point of* (1)–(2) *then the corresponding* $u^{(k)}$ *from* (2) *satisfies* (3).

Proof: Follows from the definition of $T(\cdot)$ in (A2).

Lemma 2: *Provided (A2), (A4), (A5) and (A6),* $\exists x_0 \in \mathbb{R}^n$ *such that* $x = \mathbf{1}_N \otimes x_0$ *is a fixed point of* (1)–(2).

Proof: It is sufficient to show that $\exists u_0 \in \mathbb{R}^m$ such that $u^{(k)} = \mathbf{1}_N (e_k^T u_0)$ satisfies (3), as then $x_i = x_0 = S(u_0)$ is a fixed point of (1)–(2) from Lemma 1. If u_0 satisfies

$$\begin{pmatrix} u_0^{(1)} \\ \vdots \\ u_0^{(m)} \end{pmatrix} = \begin{pmatrix} p^{(1)} T^{(1)}(u_0) \\ \vdots \\ p^{(m)} T^{(m)}(u_0) \end{pmatrix} \quad (4)$$

with $p^{(k)} \in \mathbb{R}$ from (A6) then $u^{(k)} = \mathbf{1}_N (e_k^T u_0)$ satisfies (3). Therefore, in what follows we prove that $\exists u_0 \in \mathbb{R}^m$ such that u_0 satisfies (4).

Since $T^{(k)}(u_i)$ is bounded from (A5), we have $|p^{(k)} T^{(k)}(\cdot)| \leq b^{(k)}$ for some $b^{(k)} \geq 0$. Therefore, it follows from (A4) that the function

$$F(\cdot) := \begin{pmatrix} p^{(1)}T^{(1)}(\cdot) \\ \vdots \\ p^{(m)}T^{(m)}(\cdot) \end{pmatrix}$$

is a continuous mapping of the compact convex set $\mathcal{B} := [-b^{(1)}, b^{(1)}] \times \ldots [-b^{(m)}, b^{(m)}]$ into itself (i.e., $F: \mathcal{B} \to \mathcal{B}$). Invoking the Brouwer fixed-point theorem [32] we conclude that there exists $u_0 \in \mathcal{B}$ such that $F(u_0) = u_0$, therefore, u_0 satisfies (4).

In what follows, we assume that the conditions of Lemma 2 are met, thus (1)–(2) has a homogeneous fixed point of the form $x = \mathbf{1}_N \otimes x_0$ for some $x_0 \in \mathbb{R}^n$, and let $u_0 \in \mathbb{R}^m$ denote the corresponding value of u_i for $i = 1, \ldots, N$.

3.1 Patterning with a Single Layer of Communcation

In this section, we focus on the case when $m = 1$ in (2), thus we drop the superscript.

3.1.1 Stability of the Homogeneous Fixed Points—In the following theorem, we derive a sufficient condition for the instability of the homogeneous fixed point $x = \mathbf{1}_N \otimes x_0$ relying only on the input/output function $T(\cdot)$ and on the eigenvalues of P (necessary conditions are presented in Lemma 1 in the Appendix when the linearization of (1)–(2) is also available).

Theorem 1: *Assume that (A1), (A2) and (A3) hold. The fixed point* $x = \mathbf{1}_N \otimes x_0$ *of* (1)–(2) *is unstable if P has a real eigenvalue* λ_i *such that*

$$1 - T'(u_0)\lambda_i < 0. \quad (5)$$

Proof: With

$$A := \frac{\partial f(x_i, u_i)}{\partial x_i}\Big|_{(x_0,u_0)}, \quad B := \frac{\partial f(x_i, u_i)}{\partial u_i}\Big|_{(x_0,u_0)}, \quad C := \frac{\partial h(x_i)}{\partial x_i}\Big|_{x_0}, \quad (6)$$

it is sufficient to show that (5) implies that $A + \lambda_i BC$ has an eigenvalue with positive real part according to Lemma 1 in the Appendix.

Since from [25] we obtain that $T'(u_0) = -CA^{-1}B$, (5) is equivalent to the condition $1 + \lambda_i CA^{-1}B < 0$. From Sylvester's determinant theorem it follows that

$$(-1)^n \det(A)\det(1+\lambda_i CA^{-1}B)=(-1)^n \det(A+\lambda_i BC).$$

Claim 2 in [26] yields that $(-1)^n \det(A) > 0$ since A is Hurwitz by (A3), thus we obtain that $(-1)^n \det(A+\lambda_i BC) < 0$. From this we conclude that $A + \lambda_i BC$ has a positive real eigenvalue invoking Claim 2 in [26].

3.1.2 Emergence of Patterns—Next, we study the emergence of patterns. To this end, we rely on results from the theory of monotone systems together with the notion of balanced partitioning of graphs [33]. To simplify notation, consider $M \in \mathbb{R}^{N\times N}$ and introduce

$$\Psi(M):=M-\sum_{i=1}^{N}\mathrm{diag}(e_i)M\mathrm{diag}(e_i),$$

which is the same as M except it has zeros in the diagonal.

Definition 1: The graph $\mathcal{G} = (V, W)$ is *balanced* if there is a partition of its set of nodes V into V_1 and V_2 such that all positive edges connect nodes within V_1 or V_2, and negative edges connect nodes between V_1 and V_2. Furthermore, define the *bipartition vector* $b := (b_1 \dots b_N)^T$ such that $b_i = (-1)^k$ if node i belongs to V_k $(k = 1, 2)$.

Theorem 2: *Provided (A2), (A4) and (A5), assume that the graph with irreducible adjacency matrix* $\Psi(PT'(u_0))$ *is balanced with bipartition vector b. Introduce* $u^* := \mathbf{1}_N u_0$ *and the cone* $\mathcal{K} = \{u : S(u - u^*) \geq 0\}$ *where* $S = diag(b)$. *If*

$$1-\lambda_i T'(u_0)<0 \quad (7)$$

for some real eigenvalue λ_i *of P, then both sets* $u^* \pm \mathcal{K}$ *contain a point* $u \neq u^*$ *such that* $x_i = T(u_i)$ *is a fixed point of* (1)–(2).

Proof: Introduce the auxiliary dynamical system

$$\dot{u} = -u + P \begin{pmatrix} T(u_1) \\ \vdots \\ T(u_N) \end{pmatrix} \quad (8)$$

and note that the fixed points of (8) are identical to the solutions of (3) when $m = 1$. Therefore, the fixed points of (8) are fixed points of (1)–(2) from Lemma 1. Therefore, in the rest of the proof we focus on the fixed points of (8).

First, introduce the coordinate transformation $w := Su$ and note that $S = S^{-1}$, yielding

$$\dot{w} = -w + SP \begin{pmatrix} T(b_1 w_1) \\ \vdots \\ T(b_N w_N) \end{pmatrix} =: F(w). \tag{9}$$

The Jacobian of (8) is given by $J(u) := -I + P\Delta(u)$ where $\Delta(u) := \mathrm{diag}(T'(u_1) \ldots T'(u_N))$, so that the Jacobian of (9) is given by $DF(w) := SJ(Sw)S$. We next show that (9) is *cooperative* by proving that $DF(w)$ is Metzler for all $w \in \mathbb{R}^N$. To this end, note that since the graph with irreducible adjacency matrix $\Psi(PT'(u_0))$ is balanced with bipartition vector b, so is $\Psi(P\Delta(u))$ from (A5). Therefore, we have that $b_i b_j p_{i,j} T'(u_j) \geq 0$ for $i \neq j$ and $i, j = 1, \ldots, N$. It then follows that $DF(w)$ is Metzler for all $w \in \mathbb{R}^N$, thus (9) is cooperative.

Second, we focus on the bounded forward invariant set $\mathcal{V}$ in Lemma 2 in the Appendix. From (A5) we have that $\exists \bar{T} > 0$ such that $|T(\cdot)| \leq \bar{T}$. With this, introduce $\bar{w} := \max(|u_0|, \|P\|_1 \bar{T})$ and the set $\mathcal{W} := [-\bar{w}, \bar{w}]^N$. We next show that $\mathcal{V} := S\mathcal{W}$ is forward invariant for (8). To see this, note that from (9) we obtain that

$$\dot{w}_i = -w_i + b_i \sum_{j=1}^{N} p_{i,j} T(b_j w_j),$$

where $|b_i \sum_{j=1}^{N} p_{i,j} T(b_j w_j)| \leq \|P\|_1 \bar{T}$. This yields $F_w(\bar{w}\mathbf{1}_N) \leq 0$ and $F_w(-\bar{w}\mathbf{1}_N) \geq 0$ from (9). Given that (9) is cooperative, thus monotone with respect to the standard orthant cone $\mathbb{R}^N_{\geq 0}$, we conclude that the hypercube $\mathcal{W}$ is forward invariant and it contains the equilibrium point Su^* as $\bar{w} \geq |u_0|$. Therefore, $\mathcal{V} = S\mathcal{W}$ is bounded, forward invariant and it contains u^*.

Third, note that $S^{-1}J(u^*)S = -I + S^{-1}PT'(u_0)S$. We already proved above that $D := S^{-1}PT'(u_0)S$ is Metzler. Let $d_{i,j}$ denote the entries of D $(i, j = 1, \ldots, N)$, introduce $d := \min_i d_{i,i}$ and $Q := D - dI$ together with $\alpha := 1 - d$. With this, we obtain that $S^{-1}J(u^*)S = -\alpha I + Q$ such that $Q \geq 0$ is irreducible (since P is). Therefore, to invoke Lemma 2 in the Appendix, all there is left to show is that $\rho(Q) > \alpha$.

To this end, note that the eigenvalues of D are $\lambda_j T'(u_0)$ and since D is Metzler from above, we invoke Corollary 4.3.2 in [34] to conclude that $s(D) = \lambda_i T'(u_0)$ for some i such that λ_i is real. Therefore, the condition in (7) yields that $s(D) > 1$. Furthermore, from $Q = D - dI$ it follows that $s(Q) = s(D) - d$, and since $\alpha = 1 - d$ we obtain that $s(Q) > \alpha$. Finally, from the Perron-Frobenius theorem (Theorem 4.3.1 in [34]) we have that $\rho(Q) = s(Q)$, thus $\rho(Q) > \alpha$.

Now we can invoke Lemma 2 in the Appendix with $\mathcal{V}$, S and Q defined above to conclude that both sets $u^* \pm \mathcal{K}$ contain a fixed point $u \neq u^*$ of (8). This is equivalent to having solutions u of (3) in both sets $u^* \pm \mathcal{K}$ different from u^*. Finally, we conclude from Lemma 2 that such solutions $u = (u_1 \ldots u_N)^T$ yield fixed points $x = (T(u_1) \ldots T(u_N))^T$ of (1)–(2).

3.1.3 Patterns with Groups—Finally, we search for equilibrium points of (1)–(2) in which subsystems are grouped into classes $O_1, \ldots, O_r$ such that $x_i = x_j$ if $i, j \in O_k$. Such a solution yields patterns in which subsystems of the same class have identical steady states, and it reduces the complexity of the analysis by decreasing the dimension of the problem. To find these solutions, we rely on the notion of equitable partitions of graphs [33].

Definition 2: For a weighted and directed graph (V,P) with adjacency matrix P, a partition $\boldsymbol{\pi}$ of the vertex set V into classes $O_1, \ldots, O_r$ is said to be *equitable* if there exist $\bar{p}_{i,j}$ for $i, j = 1, \ldots, r$ such that

$$\bar{p}_{i,j} = \sum_{v \in O_j} p_{u,v} \quad \forall u \in O_i. \tag{10}$$

Let the reduced adjacency matrix $\bar{P} \in \mathbb{R}^{r \times r}$ be formed by the entries $\bar{p}_{i,j}$.

Theorem 3: *Provided (A2), (A4) and (A5), let $\boldsymbol{\pi}$ be an equitable partition of the vertices V of the graph (V,P) into classes $O_1, \ldots, O_r$ and let $\bar{P}$ denote the resulting reduced adjacency matrix. Assume that $\Psi(\bar{P}T'(u_0))$ is irreducible and balanced with bipartition vector $\bar{b}$. Introduce $u^* := \mathbf{1}_r u_0$ and the cone $\mathcal{K} = \{u : S(u - u^*) \geq 0\}$ where $S = diag(b)$. If*

$$1 - \bar{\lambda}_i T'(u_0) < 0, \tag{11}$$

for some real eigenvalue $\bar{\lambda}_i$ of $\bar{P}$ then both sets $u^* \pm \mathcal{K}$ contain a point $\bar{u} \neq u^*$ such that $x_i = T(\bar{u}_j)$ for $i \in O_j$ is a fixed point of (1)–(2).

Proof: Consider the reduced set of equations

$$\begin{pmatrix} \bar{u}_1 \\ \vdots \\ \bar{u}_r \end{pmatrix} = \bar{P} \begin{pmatrix} T(\bar{u}_1) \\ \vdots \\ T(\bar{u}_r) \end{pmatrix}. \tag{12}$$

Following the same steps as in the proof of Theorem 2, we conclude that (12) has equilibrium points $\bar{u} \neq u^*$ in both sets $u^* \pm \mathcal{K}$. Exploiting the fact that $\boldsymbol{\pi}$ is an equitable partition of (V,P), a solution $\bar{u}$ of (12) also defines a solution u of (3) in which $u_i = \bar{u}_j$ for all $i \in O_j$, so that $x_i = T(\bar{u}_j)$ for $i \in O_j$, concluding the proof.

3.2 Patterning with Multiple Layers of Communication

We now focus on the case of multiple layers of communication channels ($m = 2, 3, \ldots$). In what follows, we assume that (A7) holds, thus from Theorem 1.3.19. in [35] it follows that

there exists an invertible matrix W such that $W^{-1}P^{(k)}W=\mathrm{diag}(\ \lambda_1^{(k)}\ \ \dots\ \ \lambda_N^{(k)}\ )=:\Lambda^{(k)}$ for $k = 1, \dots, m$, and define

$$\Lambda_i:=\begin{bmatrix}\lambda_i^{(1)} & & \\ & \ddots & \\ & & \lambda_i^{(m)}\end{bmatrix}\quad i=1,\dots,N. \tag{13}$$

As the proofs of theorems presented in this chapter are similar to those of the previous one for a single channel of communication, we provide them in the Appendix for the sake of brevity.

3.2.1 Stability of the Homogeneous Fixed Points—We first derive a sufficient condition for the instability of the homogeneous fixed point $x = \mathbf{1}_N \otimes x_0$ relying only on the input/output function $T(\cdot)$ and the eigenvalues of $P^{(k)}$ for $k = 1, \dots, m$ (necessary conditions are presented in Lemma 3 in the Appendix when the linearization of (1)–(2) is also available).

Theorem 4: *Assume that (A1), (A2), (A3), (A4) and (A7) hold. The fixed point* $x = \mathbf{1}_N \otimes x_0$ *of* (1)–(2) *is unstable if*

$$\det(I_m-\Lambda_i T'(u_0))<0 \tag{14}$$

for some real Λ_i *defined in* (13).

3.2.2 Emergence of Patterns—We next study the emergence of patterns and their relationship with the homogeneous fixed point $x = \mathbf{1}_N \otimes x_0$.

Theorem 5: *Assume that (A2), (A4), (A5) and (A7) hold. Furthermore, assume that the graphs with adjacency matrices* $P^{(1)}, \dots, P^{(m)}$ *are balanced with the same bipartition vector* b, *and* $T'(u_0)$ *is also balanced with bipartition vector* q. *Introduce* $u^* := \mathbf{1}_N \otimes u_0$ *and the cone* $\mathcal{K} = \{u : S(u - u^*) \geq 0\}$ *where* $S = \mathrm{diag}(b) \otimes \mathrm{diag}(q)$. *If for some* i *we have that*

$$\max_i s(\Lambda_i T'(u_0))>1, \tag{15}$$

then both sets $u^* \pm \mathcal{K}$ *contain a point* $u \neq u^*$ *such that* $x_i = T(u_i)$ *is a fixed point of* (1)–(2).

3.2.3 Patterns with Groups—Finally, we search for equilibrium points of (1)–(2) in which subsystems are grouped into classes $O_1, \dots, O_r$ such that $x_i = x_j$ if $i, j \in O_k$. Let

$\bar{P}^{(k)} \mathbb{R}^{r \times r}$ denote the reduced adjacency matrices with eigenvalues $\overline{\lambda}_i^{(k)}$ $(i=1,\ldots,r, k=1,\ldots,m)$, and define $\overline{\Lambda}_i := \mathrm{diag}(\ \overline{\lambda}_i^{(1)} \ \ldots \ \overline{\lambda}_i^{(m)}\ )$.

Theorem 6: *Assume that (A2), (A4), (A5) and (A7) hold. Let* $\boldsymbol{\pi}$ *be an equitable partition of the vertices of the graphs with adjacency matrices* $P^{(1)}, \ldots, P^{(m)}$ *into classes* $O_1, \ldots, O_r$ *for all* $k = 1, \ldots, m$. *Furthermore assume that the graphs with adjacency matrices* $\bar{P}^{(1)}, \ldots, \bar{P}^{(m)}$ *are balanced with the same bipartition vector* b, *and* $T'(u_0)$ *is also balanced with bipartition vector* q. *Introduce* $u^* := \mathbf{1}_r \otimes u_0$ *and the cone* $\mathcal{K} = \{\bar{u} : S(\bar{u} - u^*) \geq 0\}$ *where* $S = (\mathbf{1}_r b^T) \otimes (\mathbf{1}_m q^T)$. *If for some* i *we have that*

$$\max_i s(\overline{\Lambda}_i T'(u_0)) > 1,$$

then both sets $u^* \pm \mathcal{K}$ *contain a point* $\bar{u} \neq u^*$ *such that* $x_i = T(\bar{u}_j)$ *for* $i \in O_j$ *is a fixed point of* (1)–(2).

4 Application examples

We next focus on the emergence of patterns in neural networks, in reaction-diffusion systems, and in contagion processes over random networks to demonstrate how our results can be employed when studying pattern formation over networks of the form (1)–(2).

4.1 Pattern Formation in Neural Networks

Before illustrating how our results can be applied to study pattern formation over multigraphs, we first focus on pattern formation over single graphs here. In particular, consider the interconnection of N leaky integrate-and-fire neurons [36], described by

$$\begin{aligned} \dot{x}_i &= -a x_i + g(u_i), \\ y_i &= x_i, \\ u &= P y \end{aligned} \qquad (16)$$

with $a > 0$ and where $g(\cdot)$ is an increasing function such that $g(0) = 0$. In what follows, we consider

$$g(u_i) = G \frac{\exp\left(\frac{2\mu}{G} u_i\right) - 1}{\exp\left(\frac{2\mu}{G} u_i\right) + 1} \qquad (17)$$

to model the saturated nature of the interconnection channels. For simplicity, we focus on the case when $P\mathbf{1}_N = \mathbf{0}_N$ so that the origin is a fixed point of (16), thus $x_0 = u_0 = 0$.

From Lemma 4 in the Appendix it follows that the origin is globally asymptotically stable if $-a + \mu\omega_i$ has negative real part for $i = 1, \ldots, N$, where ω_i denotes the eigenvalues of the

matrix P_{abs} where $[P_{\text{abs}}]_{i,j} := |p_{i,j}|$. As a concrete example, introduce the asymmetric interconnection matrix

$$P = \begin{bmatrix} 1 & -1 & & \\ & \ddots & \ddots & \\ & & \ddots & -1 \\ -1 & & & 1 \end{bmatrix}, \tag{18}$$

describing the interconnection of N neurons in a ring structure such that each neuron activates itself and inhibits its neighbor on the right-hand side, and assume that N is even. Lemma 4 in the Appendix then yields that the origin is a globally asymptotically stable fixed point of (16)–(18) if $\mu < a/2$ (left panel in Fig. 1).

Building on the results presented in Section III.A, we first show that an alternating pattern (right panel in Fig. 1) of the form $x_1 = -x_2 = x_3 = \ldots = x_{N-1} = -x_N \neq 0$ emerges when $\mu > a/2$. Then we prove that this pattern is unique (up to rotation along the ring) and stable.

Invoking Theorem 3, we first prove that (16)–(18) has two fixed points other than the origin: one such that $x_{2k-1} \geq 0$ and $x_{2k} \leq 0$; and another such that $x_{2k-1} \leq 0$ and $x_{2k} \geq 0$ for $k = 1, \ldots, N/2$. To this end, note first that the partition π of the vertices into $O_1 = \{1, 3, \ldots, N-1\}$ and $O_2 = \{2, 4, \ldots, N\}$ is equitable. The eigenvalues of the corresponding reduced adjacency matrix

$$\overline{P} = \begin{bmatrix} 1 & -1 \\ -1 & 1 \end{bmatrix}$$

are $\bar{\lambda}_1 = 0$ and $\bar{\lambda}_2 = 2$. Second, the irreducible matrix

$$\Psi(\overline{P}T'(u_0)) = \begin{bmatrix} 0 & -\mu/a \\ -\mu/a & 0 \end{bmatrix}$$

is balanced with bipartition vector $\bar{b} = (1\ -1)^T$. Third, since $u_0 = 0$, we obtain that $u^* := \mathbf{1}_N u_0$ is the origin, yielding the cone $\mathcal{K} := \{\bar{u} : \operatorname{diag}(\bar{b})(\bar{u} - u^*) \geq 0\} = \{\bar{u} : \bar{u}_1 \geq 0, \bar{u}_2 \leq 0\}$. Therefore, from Theorem 3 it follows that if $\mu > a/2$ then there exist $\bar{u}_1 \geq 0$ and $\bar{u}_2 \leq 0$ not simultaneously zero such that for $i = 1, \ldots, N$ both

$$x_i = \begin{cases} T(\bar{u}_1) & i \text{ even} \\ T(\bar{u}_2) & i \text{ odd} \end{cases} \tag{19}$$

and

$$x_i = \begin{cases} T(\bar{u}_1) & i \text{ odd} \\ T(\bar{u}_2) & i \text{ even} \end{cases} \quad (20)$$

are fixed points of (16)–(18), where $T(\bar{u}_1) \geq 0$ and $T(\bar{u}_2) \leq 0$ are not simultaneously zero.

Next, we prove that apart from the origin, the only fixed points of (16)–(18) are those in (19)–(20). To this end, consider first the unique solution $x^* > 0$ of

$$x^* = \frac{G}{a} \frac{\exp(\frac{4\mu}{G} x^*) - 1}{\exp(\frac{4\mu}{G} x^*) + 1} \quad (21)$$

and note that with $\bar{u}_1 := 2x^* > 0$ and $\bar{u}_2 := -2x^* < 0$ we have $x^* = T(\bar{u}_1) > 0$ and $-x^* = T(\bar{u}_2) < 0$. Since $|g(u_i)| < G$ we have that $\dot{x}_i$ can only be zero if $|x_i| < G/a$, therefore, what is left to show is that if $x_i \in (0, x^*)$ or $x_i \in (x^*, G/a)$ then x can not be a fixed point of (16)–(18). To this end, note that

$$x_{i+1} = x_i + \frac{G}{2\mu} \ln \left(\frac{\frac{G}{a} - x_i}{\frac{G}{a} + x_i} \right) =: M(x_i), \quad (22)$$

so that for x to be a fixed point we must have that

$$x_i = (\underbrace{M \circ M \circ \cdots \circ M}_{N})(x_i).$$

From (22) it follows that $|M(x^*)| = x^*$ and we obtain that $|M(x_i)| < x_i$ for $|x_i| < x^*$ and $|M(x_i)| > x_i$ for $x^* < |x_i| < G/a$. Therefore, we must have $|x_i| = x^*$ for x to be a fixed point, and then from (22) it follows that either $x_i = (-1)^i x^*$ or $x_i = (-1)^{i+1} x^*$ for $i = 1, 2, \ldots, N$.

Finally, we show that the alternating patterns in (19)–(20) are stable fixed points of (16)–(18). To this end, define $\alpha := 2\mu/a$ and $v := 2ax^*/G$ such that from (21) we have that $v = (e^{2\alpha v} - 1)/(e^{2\alpha v} + 1)$, and let $v = V(\alpha)$ denote its positive solution. Define $h(\alpha) := 2\alpha e^{\alpha V(\alpha)}/[(e^{2\alpha V(\alpha)} + 1)^2]$, yielding $g'(\bar{u}_1) = g'(\bar{u}_2) = g'(\pm 2x^*) = ah(\alpha)$. Since $0 < h(\alpha) < 0.5$ for $\alpha > 1$ (verified numerically), this then implies that with $\tilde{P} := ah(\alpha)P$ its spectral radius $\rho(\tilde{P})$ is such that $\rho(\tilde{P}) = ah(\alpha)\rho(P) < a$. Lemma 5 in the Appendix then yields that the alternating patterns in (19)–(20) are stable fixed point of (16)–(18).

4.2 Pattern Formation in Reaction-Diffusion Networks

We first briefly illustrate the idea underlying diffusion-driven pattern formation considering the system

$$\begin{aligned}\dot{x}_{i,1}&=ax_{i,1}+bx_{i,2},\\ \dot{x}_{i,2}&=-cx_{i,1}-dx_{i,2}+g(u_i),\\ y_i&=x_{i,2},\\ u&=Py,\end{aligned} \tag{23}$$

such that $a, b, c, d > 0$, $g(0) = 0$ and $g'(\cdot) > 0$; for instance, see (17). The unconnected systems ($P = 0$) are stable at the origin if $ad - bc < 0$ and $a < d$, but can become unstable when interconnected. As a concrete example, consider the interconnection matrix

$$P=\begin{bmatrix}-2 & 1 & & 1\\ 1 & \ddots & \ddots & \\ & \ddots & \ddots & 1\\ 1 & & 1 & -2\end{bmatrix}. \tag{24}$$

From Lemma 4 in the Appendix it follows that the origin is stable if $g'(0) < (a - d)/4$, and conversely, it becomes unstable when $g'(0) > (a - d)/4$. As previously, we can study the emergence of various patterns invoking Theorem 3. For instance, the partition π of the vertices into $O_1 = \{1, 3, \ldots, N-1\}$ and $O_2 = \{2, 4, \ldots, N\}$ is equitable, so that following a similar reasoning as in the previous example, we expect the emergence of an alternating pattern, verified in Fig. 2. The stability of various patterns can be analyzed using Lemma 5 in the Appenidx, as demonstrated in the previous example.

Having illustrated diffusion-driven pattern formation on the idealized system in (23), we next focus on the Brusselator [37], a standard biochemical model for Turing pattern formation (other models, such as that of Gierer and Meinhardt [4], of Schnakenberg [38], and of Thomas [39] can be treated similarly). We demonstrate how our results can be used in the case of multigraphs, and illustrate that considering different interconnection structures for different species can decrease the often prohibitively large difference in diffusion coefficients required for pattern formation.

Consider first the non-dimensional model of an isolated Brusselator given by

$$\begin{aligned}\dot{x}_{i,1}&=1-(1+b)x_{i,1}+ax_{i,1}^2x_{i,2},\\ \dot{x}_{i,2}&=bx_{i,1}-ax_{i,1}^2x_{i,2},\end{aligned} \tag{25}$$

where $a, b > 0$. It follows from linearization about the steady state $x = (1, b/a)^T$ that the unique fixed point is stable if $b < a + 1$.

Upon interconnection, the dynamics of the network become

$$\begin{aligned}
\dot{x}_{i,1} &= 1-(1+b)x_{i,1}+ax_{i,1}^2x_{i,2}+g_1(u_i^{(1)}),\\
\dot{x}_{i,2} &= bx_{i,1}-ax_{i,1}^2x_{i,2}+g_2(u_i^{(2)}),\\
y_{i,j} &= x_{i,j} \quad j=1,2,\\
u^{(j)} &= P^{(j)}y^{(j)} \quad j=1,2
\end{aligned} \tag{26}$$

with $g_i(\cdot)$ from (17). Since $g_i(0) = 0$ and $P^{(i)}\mathbf{1}_N = \mathbf{0}_N$, we obtain $u_0 = (0, 0)^T$ at the homogeneous steady state. Next, we study the stability of this fixed point.

Define $\omega_i^{(j)} := -g_j'(0)\lambda_i^{(j)}$. Then, from (26) Lemma 6 in the Appendix it follows that $x = \mathbf{1}_N \otimes x_0$ is unstable if for some $i \in \{1, \ldots, N\}$ we have

$$b > 1 + a\frac{1+\omega_i^{(1)}}{\omega_i^{(2)}} + \omega_i^{(1)}, \tag{27}$$

and stable otherwise. Since $g_j'(0) > 0$ and $\lambda_i^{(1)} \leq 0$, we have that $\omega_i^{(j)} \geq 0$ for $j = 1, 2$ and $i = 1, \ldots, N$. For instance, consider the case when $P^{(1)} = P^{(2)} = P$ with P from (24), so that $\lambda_N^{(1)} = \lambda_N^{(2)} = -4$. Considering the parameters $a = 1$, $b = 1.8$, and $\mu_2/\mu_1 = 21$ from [40], we need to have $\mu_1 > 0.0174$ to satisfy (27). When $\mu_1 < 0.0174$, the homogeneous steady state is stable (Fig. 3, top panels), conversely, a pattern emerges when μ_1 becomes greater than 0.0174 (Fig. 3, bottom panels).

Next, we illustrate how we can leverage different interconnection structures for different species to decrease the often prohibitively large difference in diffusion coefficients required for pattern formation. To this end, note first that (27) reveals that $b > 1$ is necessary for $x = \mathbf{1}_N \otimes x_0$ to become unstable, so that in what follows we consider this to be the case. Assume that (27) is satisfied for some i, and introduce $\varepsilon := \omega_i^{(2)}/\omega_i^{(1)}$. Then from (27) it follows that we must have $\varepsilon > a(1+\sqrt{b})^2/(1-b)^2 =: \varepsilon^*$ for $x = \mathbf{1}_N \otimes x_0$ to become unstable. If the interconnection matrices are identical, i.e., $P^{(1)} = P^{(2)}$, then $\lambda_i^{(1)} = \lambda_i^{(2)}$ for $i = 1, 2, \ldots, N$, yielding $\varepsilon^* = \mu_2/\mu_1$. Since $\varepsilon^* > 1$, we have that $\mu_2 > \mu_1$, thus the diffusibility of the inhibitor $x_{i,2}$ dominates that of the activator $x_{i,1}$, hence Turing instability is often referred to as "local activation with long range inhibition."

Since $\varepsilon^* = \mu_2/\mu_1$ can be much greater than 1, especially when $b \approx 1$, this often presents experimental challenges in synthetic biology. To overcome this obstacle, it is possible to artificially decrease the diffusion coefficient of the activator by introducing a third molecule

binding to the activator, thus rendering it effectively inactive [41]. Instead of adding this molecule to all the physical channels among nodes, we can further decrease ε by adding this molecule only to a few select physical channels, thus introducing different interconnection matrices for activator and inhibitor (i.e., $P^{(1)} \neq P^{(2)}$), yielding different eigenvalues $\lambda_i^{(1)}$ and $\lambda_i^{(2)}$ for $i = 1, \ldots, N$.

To illustrate this, let $\lambda_N^{(j)}$ denote the smallest (largest in absolute value) eigenvalue of $P^{(j)}$ for $j = 1, 2$, and assume that (27) holds for $i = N$, thus the fixed point is unstable. This means that $(\mu_2\lambda_N^{(2)})/(\mu_1\lambda_N^{(1)}) > \varepsilon^*$, so that if $\lambda_N^{(2)} > \lambda_N^{(1)}$ then it is sufficient to have $\mu_2/\mu_1 > \varepsilon^*\lambda_N^{(1)}/\lambda_N^{(2)} =: \tilde{\varepsilon}$ such that $\tilde{\varepsilon} < \varepsilon^*$. For instance, consider first the case when $P^{(1)} = P^{(2)} = P$ with P from (24), so that $\lambda_N^{(1)} = \lambda_N^{(2)} = -4$. Next, rewiring the network for the activators $x_{i,1}$ such that the corresponding interconnection matrix becomes $P^{(1)} := ([P^{(2)}]^2 + 6P^{(2)})/3$ yields $\lambda_N^{(1)} = -3$ (as $N \to \infty$). This means that $\tilde{\varepsilon} = 0.75\varepsilon^*$, thus the required difference between diffusion coefficients is now reduced by 25%.

4.3 Contagion Processes over Random Graphs

Finally, we discuss pattern formation in connected random networks, illustrated considering contagion processes. Here we focus on two of the most common network models: Erdos-Renyi random graphs [42] and scale-free networks generated by preferential attachment [43] (other network models can be anayzed similarly). Considering the symmetric and irreducible Laplacian matrix P associated with the network structure, we have that $\rho(P) = s(P) = \lambda_{\max} > 0$ where $\lambda_{\max}$ is the dominant eigenvalue of P (Theorem 4.3.1 in [34]), a quantity that plays a central role in pattern formation.

In Fig. 4 we display the dominant eigenvalue $\lambda_{\max}$ of P for various network sizes as a function of density. According to these results, $\lambda_{\max}$ is heavily influenced by how the random network is generated: it is significantly larger in the case of scale-free networks than in Erdos- Renyi random graphs. To illustrate what this means in the context of pattern formation, we next fix the network size ($N = 200$) and consider two networks generated by the above two methods with the same density (5%). The dominant eigenvalue $\lambda_{\max}$ of the Laplacian matrices associated with these two networks differ significantly: $\lambda_{\max}^{\mathrm{SF}} \approx 50$ and $\lambda_{\max}^{\mathrm{ER}} \approx 20$ for scale-free networks and Erdos-Renyi random graphs, respectively, in accordance with the results depicted in Fig. 4.

As for nodal dynamics, we consider one of the standard compartmental models in epidemiology: the SIS model given by

$$\begin{aligned} \dot{x}_{i,1} &= \alpha - \beta x_{i,1}x_{i,2} + \gamma x_{i,2} - \delta x_{i,1} + g(u_i), \\ \dot{x}_{i,2} &= \alpha + \beta x_{i,1}x_{i,2} - \gamma x_{i,2} - \delta x_{i,2}, \end{aligned} \tag{28}$$

for $i = 1, \ldots, N$, where α, β, γ, and δ are the birth, infection, revocery, and death rates, respectively [44]. In this model, $x_{i,1}$ and $x_{i,2}$ denote the number of susceptible and infected (e.g., with flu) agents in population i, respectively.

From (17) we obtain that $g(u_i) \equiv 0$ when $\mu = 0$, thus the nodes in the network are effectively not interconnected, so that trajectories of (28) converge to the homogeneous fixed point $x = \mathbf{1}_N \otimes x_0$ where $x_0 = (x_{0,1}, x_{0,2})^T$. In the simulations we consider $\alpha = \beta = 1$ and $\gamma = \delta = 10$, yielding $x_{0,1} = x_{0,2} = 1$. According to Theorem 2, once (7) is satisfied, the homogeneous fixed point becomes unstable, thus giving rise to patterning. With $g(u_i)$ from (17) we obtain that $T'(u_0) = \mu 11$ with $\alpha = \beta = 1$ and $\gamma = \delta = 10$. Therefore, since $\lambda_{\max}^{\mathrm{ER}} < \lambda_{\max}^{\mathrm{SF}}$, from (7) we expect no patterning when $\mu \in [0, {}^{11}\!\Big/\!_{\lambda_{\max}^{\mathrm{SF}}}) \approx [0, 0.22)$, patterning only in the scale-free network for $\mu \in ({}^{11}\!\Big/\!_{\lambda_{\max}^{\mathrm{SF}}}, {}^{11}\!\Big/\!_{\lambda_{\max}^{\mathrm{ER}}}) \approx (0.22, 0.55)$, and patterning in both networks when $\mu > {}^{11}\!\Big/\!_{\lambda_{\max}^{\mathrm{ER}}} \approx 0.55$, verified in Fig. 5.

Finally, to interpret the above results, note that P is symmetric, thus $\lambda_{\max} = \sigma_{\max}$ where $\sigma_{\max}$ is the largest singular value of P. From this, the induced 2-norm of P is $\|P\|_2 = \max_{\|z\|_2=1} \|Pz\|_2 = \sigma_{\max} = \lambda_{\max} = \rho(P)$. Let $d_{\max}$ denote the maximum vertex degree and assume that the vertex degree of node i is $d_{\max}$. Let $z^* \in \mathbb{R}_N$ be such that $z_j = 1/d_{\max}$ if $p_{i,j} = 1$ (nodes i and j are neighbors) and zero otherwise, so that $\|z\|_2 = 1$. From this we obtain that $\rho(P) = \|P\|_2 \geq d_{\max}$. The maximum vertex degree is usually (much) greater in the case of preferential attachment than in case of Erdos-Renyi random graphs (with the same density), in turn providing a (much) greater lower bound for the spectral radius $\rho(P)$, elucidating the simulation results in Fig. 4, and as a result, those in Fig. 5.

5 Discussion

In this paper, we presented analytical results for pattern formation in large-scale networks. Our results are applicable to multigraphs having multiple layers of communication channels with possibly different interconnection structure for these layers, and we allow for asymmetric connections between nodes. Furthermore, by placing no restriction on the row-sum of the interconnection matrices, our results apply to a wide set of mechanisms leading to patterning (e.g., diffusion-driven instability and lateral inhibition). Therefore, the results presented here significantly advance our understanding of patterning in a general setting by overcoming the dimensional constraints of earlier studies.

By relying only on the static input/output characteristic of each module and the algebraic properties of the interconnection matrices, we first characterized the stability of the homogeneous fixed points. Following this, we provided sufficient conditions for the emergence of non-homogeneous patterns for balanced graphs and demonstrated that equitable partitions provide templates for patterns such that modules share the same fate within partitions. Finally, we illustrated our results in the context of neural networks, of reaction-diffusion systems, and of contagion processes over random graphs.

Within our formulation, we allowed for directed edges between nodes, different topologies for different layers of communication channels, and we placed no restriction on the row-sum of the interconnection matrices. Because of this general formulation, the practical applications of our results span many fields where the emergence of patterns is a central topic of interest. For instance, we demonstrated that considering different interconnection structures for different species in reaction-diffusion networks can be leveraged to decrease the often prohibitively large difference in diffusion coefficients required for pattern formation. This result can provide insight when studying self-organization in developmental biology [45] as well as guide the design of population-level behavior in synthetic biology [46]. Additionally, we illustrated not only that random networks with the same density can behave drastically differently in terms of patterning, but more importantly, that this difference can be understood by focusing on the dominant eigenvalue of the interconnection matrix. In addition to being relevant when focusing on the spreading of infectious diseases and the behavior of multiple connected habitats in ecology [47], this result is especially well-suited for studying social networks to understand, for instance, racial segregation in sociology [48] and the polarization of opinions in political science [49]. Finally, our results apply equally to different mechanisms underlying pattern formation (diffusion, averaging, lateral inhibition, etc.), both for the diffusion of matter (zero row-sum due to conservation laws [27], [28], [29], [30], [31]) and for the diffusion of opinions (non-zero row-sum due to lack of conservation laws [25], [26]), further broadening the applicability of our results and their practical implications.

The two most limiting assumptions of the results presented here concern the interconnection structure. First and foremost, to leverage results from monotone systems theory to conclude the emergence of non-homogeneous steady state patterns we relied on the fact that the graphs representing the connections among modules are balanced. To overcome this limitation, a generalization to a larger class of graphs needs to be developed. Second, in the case of multiple layers of communication channels, we assumed that the set of interconnection matrices $P^{(1)}, \ldots, P^{(m)}$ commute. This allowed us to simultaneously diagonalize these matrices, thus significantly decrease the difficulty of analyzing the emergence of patterns. While this assumption is not overly restrictive in biological systems, where the interconnection channels are often identical for all species, it might not be the case in other contexts. For instance, in social networks different types of ties can have fundamentally dissimilar underlying interconnection structure. While a set of commuting adjacency matrices allow for complex interconnection structures, to broaden the applicability of our results this assumption needs to be weakened.

Supplementary Material

Refer to Web version on PubMed Central for supplementary material.

Acknowledgments

This work is supported in part by the grants NIH NIGMS 1R01GM109460-01 and AFOSR FA9550-14-1-0089.

References

1. Gilbert, SF. Developmental Biology. 9. Sunderland, MA: Sinauer Associates; 2010.
2. Wolpertand, L., Tickle, C. Principles of Development. 4. London, UK: Oxford University Press; 2011.
3. Turing AM. The chemical basis of morphogenesis. Philosophical Transactions of the Royal Society of London. 1952; 237:37–72.
4. Gierer A, Meinhardt H. A theory of biological pattern formation. Kybernetik. 1972; 12:30–39. [PubMed: 4663624]
5. Dillon R, Maini PK, Othmer HG. Pattern formation in generalized turing systems. Journal of Mathematical Biology. 1994; 32:345–393.
6. Murray, JD. Mathematical Biology II: Spatial Models and Biomedical Applications. New York, NY: Springer; 2003.
7. Horvath J, Szalai I, Kepper PD. An experimental design method leading to chemical turing patterns. Science. 2009; 324:772–775. [PubMed: 19423823]
8. Tompkins N, Li N, Girabawe C, Heymann M, Ermentrout GB, Epstein IR, Fraden S. Testing turings theory of morphogenesis in chemical cells. PNAS. 2013; 111:4397–4402.
9. Kouvaris NE, Sebek M, Mikhailov AS, Kiss IZ. Self-organized stationary patterns in networks of bistable chemical reactions. Angewandte Chemie International Edition. 2016; 55:13 267–13 270.
10. Bullara D, Decker YD. Pigment cell movement is not required for generation of turing patterns in zebrafish skin. Nature Communications. 2015; 6(6971) doi:10.1038.
11. Collier JR, Monk NA, Maini PK, Lewis JH. Pattern formation by lateral inhibition with feedback: A mathematical model of delta-notch intercellular signalling. Journal of Theoretical Biology. 1996; 183:429–446. [PubMed: 9015458]
12. Sprinzak D, Lakhanpal A, Bon LL, Santat L, Fontes M, Anderson G, Garcia-Ojalvo J, Elowitz M. Cis-interactions between notch and delta generate mutually exclusive signalling states. Nature. 2010; 465:86–90. [PubMed: 20418862]
13. Sprinzak D, Lakhanpal A, Bon LL, Garcia-Ojalvo J, Elowitz M. Mutual inactivation of notch receptors and ligands facilitates developmental patterning. PLoS Computational Biology. 2011; 7(6)
14. Aoki K, Diner E, de Roodenbeke C, Burgess B, Poole S, Braaten B, Jones A, Webb J, Hayes C, Cotter P, Low D. A widespread family of polymorphic contact-dependent toxin delivery systems in bacteria. Nature. 2010; 468:439–442. [PubMed: 21085179]
15. Hanski I. Metapopulation dynamics. Nature. 1998; 396:41–49.
16. Fortuna MA, Gomez-Rodriguez C, Bascompte J. Spatial network structure and amphibian persistence in stochastic environments. Proceedings of the Royal Society B: Biological Sciences. 2006; 273:1429–1434. [PubMed: 16777733]
17. Pastor-Satorras R, Vespignani A. Epidemic spreading in scale-free networks. Physical Review Letters. 2001; 86:3200–3203. [PubMed: 11290142]
18. Hufnagel L, Brockmann D, Geisel T. Forecast and control of epidemics in a globalized world. PNAS. 2004; 101:15 124–15 129.
19. Colizza V, Barrat A, Barthelemy M, Vespignani A. The role of the airline transportation network in the prediction and predictability of global epidemics. PNAS. 2006; 103:2015–2020. [PubMed: 16461461]
20. Othmer HG, Scriven LE. Instability and dynamic pattern in cellular networks. Journal of Theoretical Biology. 1971; 32:507–537. [PubMed: 5571122]
21. Othmer HG, Scriven LE. Non-linear aspects of dynamic pattern in cellular networks. Journal of Theoretical Biology. 1974; 43:83–112. [PubMed: 4813541]
22. Horsthemkea W, Lamb K, Moore PK. Network topology and turing instabilities in small arrays of diffusively coupled reactors. Physics Letters A. 2004; 328:444–451.
23. Moore PK, Horsthemkea W. Localized patterns in homogeneous networks of diffusively coupled reactors. Physica D: Nonlinear Phenomena. 2005; 206:121–144.

24. Ghosh R, Tomlin JC. Symbolic reachable set computation of piecewise affine hybrid automata and its application to biological modeling: Delta-notch protein signaling. IET Systems Biol. 2004; 1:170–183.
25. Arcak M. Pattern formation by lateral inhibition in large-scale networks of cells. IEEE Transactions on Automatic Control. 2013; 58(5):1250–1262.
26. Ferreira ASR, Arcak M. A graph partitioning approach to predicting patterns in lateral inhibition systems. SIAM Journal on Applied Dynamical Systems. 2013; 12(4):2012–2031. [PubMed: 29225552]
27. Asllani M, Challenger JD, Pavone FS, Sacconi L, Fanelli D. The theory of pattern formation on directed networks. Nature Communications. 2014; 5(4517) doi:10.1038.
28. Tang L, Wu X, Lü J, Lu J-a, D'Souza RM. Master stability functions for multiplex networks. Nov. 2016 ArXiv e-prints.
29. Asllani M, Busiello DM, Carletti T, Fanelli D, Planchon G. Turing patterns in multiplex networks. Physical Review E. 2014; 90(4)
30. Kouvaris NE, Hata S, Guilera AD. Pattern formation in multiplex networks. Scientific Reports. 2015; 5:10840. [PubMed: 26042606]
31. Brechtel A, Gramlich P, Ritterskamp D, Drossel B, Gross T. Master stability functions reveal diffusion-driven instabilities in multi-layer networks. Oct.2016 ArXiv e-prints.
32. Brouwer LEJ. Uber abbildungen von mannigfaltigkeiten. Mathematische Annalen. 1911; 71:97–115.
33. Bollobas, B. Modern Graph Theory. New York, NY: Springer; 1998.
34. Smith, HL. Mathematical Surveys and Monographs. Vol. 41. Providence, RI: American Mathematical Society; 1995. Monotone dynamical systems: An introduction to the theory of competitive and cooperative systems.
35. Horn, RA., Johnson, CR. Matrix Analysis. Cambridge, UK: Cambridge University Press; 1990.
36. Koch, C., Segev, I. Methods in neuronal modeling: from ions to networks. 2. Cambridge, MA: MIT Press; 1999.
37. Lefever R, Nicolis G. Chemical instabilities and sustained oscillations. Journal of Theoretical Biology. 1971; 30:267–284. [PubMed: 5548027]
38. Schnakenberg J. Simple chemical reaction systems with limit cycle behaviour. Journal of Theoretical Biology. 1979; 81:389–400. [PubMed: 537379]
39. Thomas, D., Kernevez, JP. Analysis and control of immobilized enzyme systems. New York, NY: Springer-Verlag; 1995.
40. Nakao H, Mikhailov AS. Turing patterns in network-organized activatorinhibitor systems. Nature Physics. 2010; 6:544–550.
41. Lengyel I, Epstein IR. Modeling of turing structures in the chlorite–iodide–malonic acid–starch reaction system. Science. 1991; 251(4994):650–652. [PubMed: 17741380]
42. Erdos P, Renyi A. On random graphs. i. Publicationes Mathematicae. 1959; 6:290–297.
43. Albert R, Barabasi AL. Statistical mechanics of complex networks. Reviews of Modern Physics. 2002; 74(1):47–97.
44. Levin, SA., Gross, LJ., Hallam, TG. Applied Mathematical Ecology. Berlin, Germany: Springer-Verlag; 1989.
45. Koch AJ, Meinhardt H. Biological pattern formation: from basic mechanisms to complex structures. Reviews of Modern Physics. 1994; 66
46. Borek B, Hasty J, Tsimring L. Turing patterning using gene circuits with gas-induced degradation of quorum sensing molecules. PLoS One. 2016; 11
47. Eisinger D, Thulke HH. Spatial pattern formation facilitates eradication of infectious diseases. Journal of Applied Ecology. 2008; 45(2):415–423. [PubMed: 18784795]
48. Clark WAV, Fossett M. Understanding the social context of the schelling segregation model. Proceedings of the National Academy of Sciences. 2008; 105(11):4109–4114.
49. Druckman JN, Peterson E, Slothuus R. How elite partisan polarization affects public opinion formation. American Political Science Review. 2013; 107(1):57–79.

Biographies

Andras Gyorgy received M.S. degrees both in Electrical Engineering and in Biomedical Engineering in 2009 and 2011, respectively, both from the Budapest University of Technology and Economics, Hungary. He then received the Ph.D. degree from the Massachusetts Institute of Technology in 2016. He is currently a postdoctoral researcher at the University of California, Berkeley. His research is in dynamical systems and control theory with applications to biological networks in synthetic and systems biology.

Murat Arcak received the B.S. degree from the Bogazici University, Istanbul, in 1996 and the M.S. and Ph.D. degrees from the University of California, Santa Barbara, in 1997 and 2000, respectively. He is currently a professor at U.C. Berkeley in the Electrical Engineering and Computer Sciences Department. His research is in dynamical systems and control theory with applications to synthetic biology, multi-agent systems, and transportation. He received the Donald P. Eckman Award from the American Automatic Control Council in 2006, the Control and Systems Theory Prize from the Society for Industrial and Applied Mathematics (SIAM) in 2007, and the Antonio Ruberti Young Researcher Prize from the IEEE Control Systems Society in 2014. He is a member of SIAM and a fellow of IEEE.

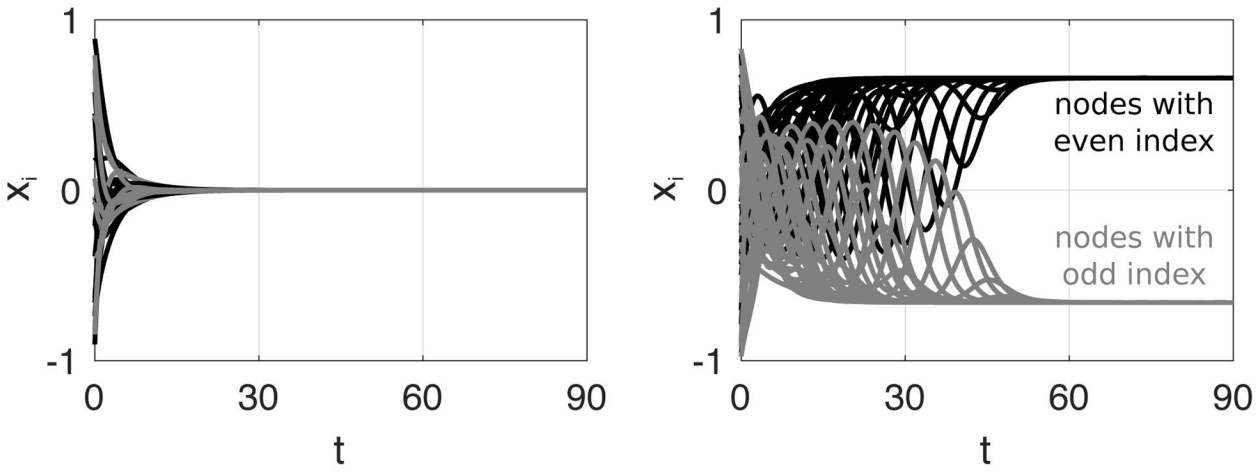

Fig. 1.

Pattern formation in neural networks. The origin is globally asymptotically stable when $\mu < a/2$ (left panel, simulation parameters: $N = 50$, $a = 1$, $G = 1$, $\mu = 0.4$). A unique alternating steady state pattern emerges when $\mu > a/2$ (right panel, simulation parameters: $N = 50$, $a = 1$, $G = 1$, $\mu = 0.4$).

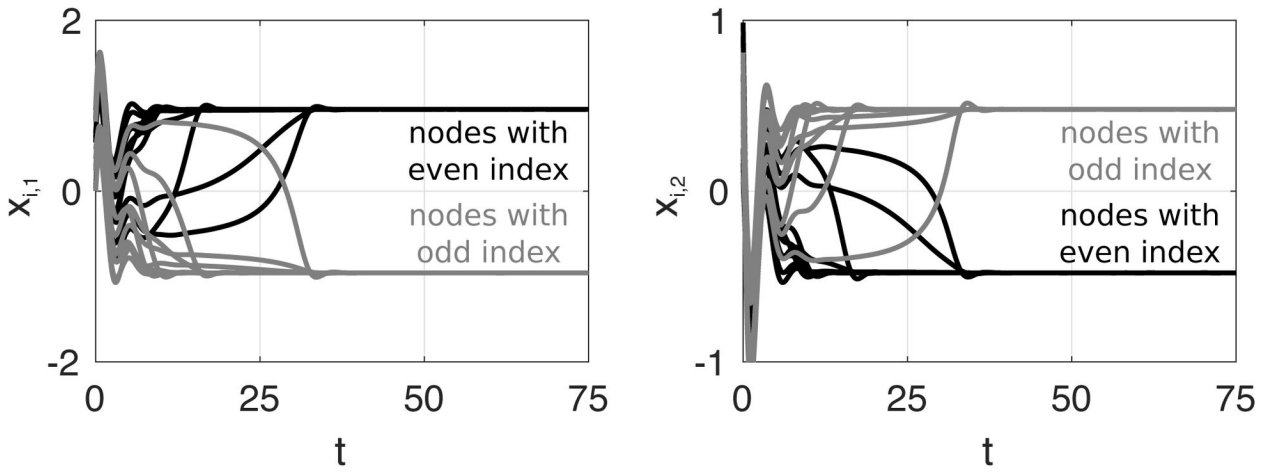

Fig. 2.

Pattern formation in reaction-diffusion networks. Once $g'(0) > (a - d)/4$, the origin becomes unstable and patterns emerge, for instance, the alternating pattern in which subsequent nodes have alternating fates along a ring (simulation parameters: $a = G = \mu = 1$, $b = c = d = 2$, $N = 20$.)

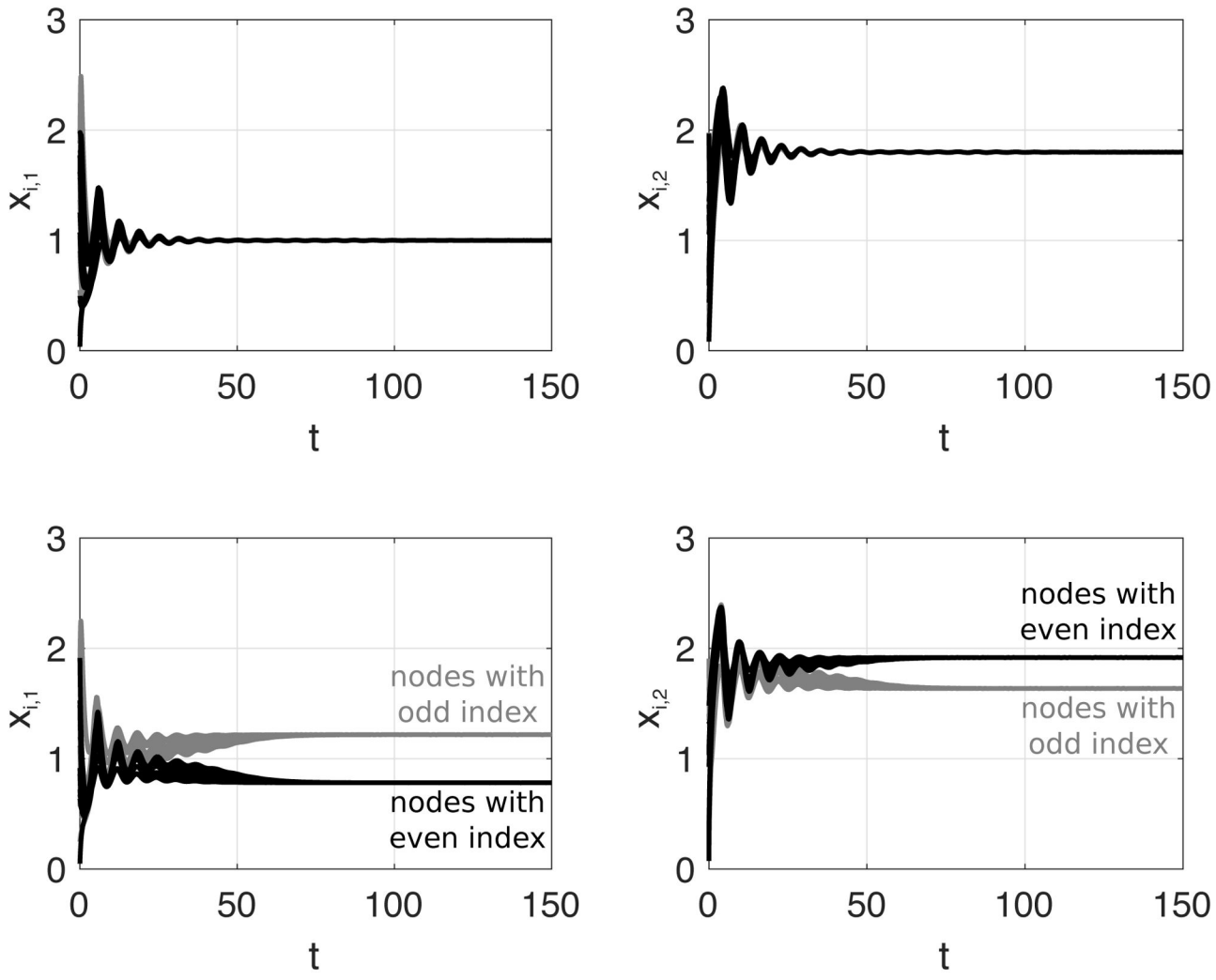

Fig. 3.

Emergence of patterns with $N = 20$ Brusselators interconnected in a ring structure. When $\mu_1 < 0.0174$, the homogeneous steady state is stable ($\mu_1 = 0.015$ in the top panels). When μ_1 becomes greater than 0.0174, the homogeneous steady state becomes unstable and a pattern emerges: an alternating one in this particular simulation ($\mu_1 = 0.02$ in the bottom panels).

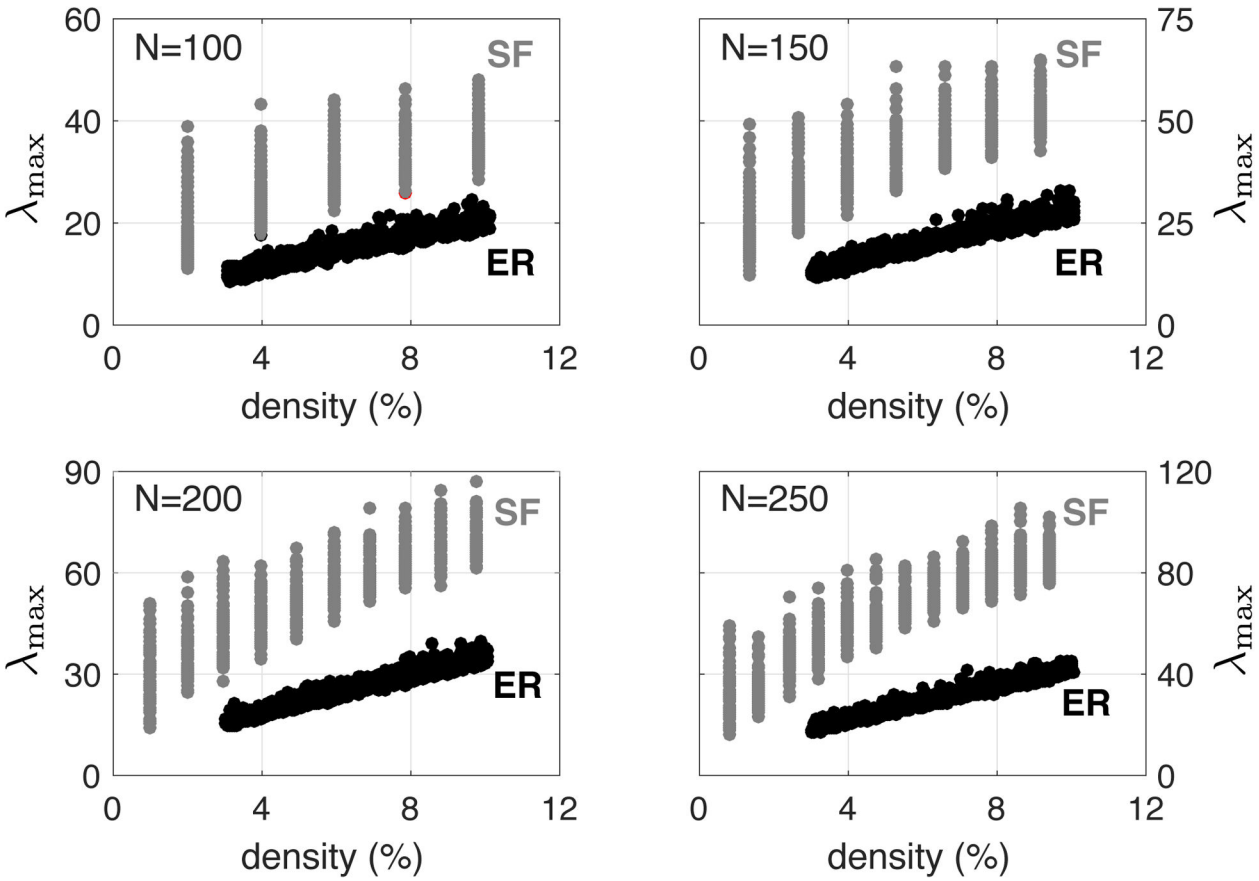

Fig. 4.

The dominant egienvalue λ_{max} of the Laplacian associated with the network structure is greater in scale-free networks (SF) than in Erdos-Renyi random graphs (ER) of the same density.

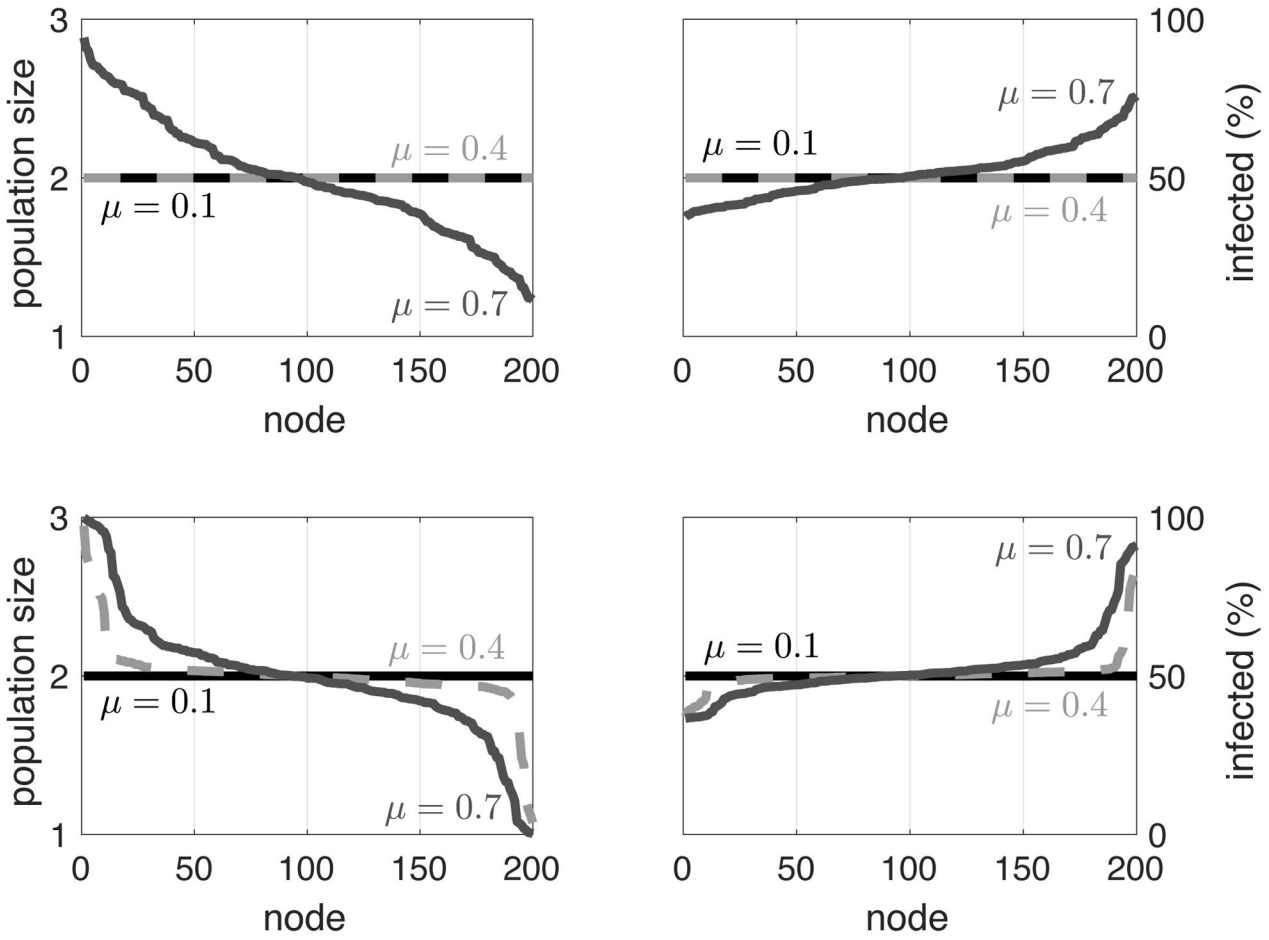

Fig. 5.

Pattern formation with SIS nodal dynamics over an Erdos-Renyi random graph (top panels) and over a scale-free random network generated by preferential attachment (bottom panels). Both networks have $N = 200$ nodes and density of 5%. When μ is sufficiently small such that (7) is not satisifed, both the population size $x_{i,1}+x_{i,2}$ for each node and the infected fraction $x_{i,2}/(x_{i,1}+x_{i,2})$ of the population are the same for all nodes. Once μ is greater than the critical threshold $\mu^* \propto 1/\lambda_{\max}$ such that (7) is satisfied, the homogeneous fixed point becomes unstable and patterns emerge. Since $\lambda_{\max}$ is greater in scale-free networks than in Erdos-Renyi random graphs (Fig. 4), the critical threshold μ^* is smaller for the former. Simulation parameters: $\alpha = \beta = 1$, $\gamma = \delta = G = 10$, together with $\mu = 0.1$ (black), $\mu = 0.4$ (dashed light grey), and $\mu = 0.7$ (solid dark grey).